TOPFARM: Multi-fidelity optimization of wind farms

Réthoré, Pierre-Elouan; Fuglsang, Peter; Larsen, Gunner Chr.; Buhl, Thomas; Larsen, Torben J.; Aagaard Madsen , Helge

Published in:
Wind Energy

Link to article, DOI:
10.1002/we.1667

Publication date:
2014

Document Version
Publisher's PDF, also known as Version of record

Wind Energy

WIND ENERGY
Wind Energ. (2013)
Published online in Wiley Online Library (wileyonlinelibrary.com). DOI: 10.1002/we.1667

RESEARCH ARTICLE

TOPFARM: Multi-fidelity optimization of wind farms

Pierre-Elouan Réthoré, Peter Fuglsang, Gunner C. Larsen, Thomas Buhl, Torben J. Larsen and Helge A. Madsen

Wind Energy Department, DTU, Risø Campus, DK-4000 Roskilde, Denmark

ABSTRACT

A wind farm layout optimization framework based on a multi-fidelity optimization approach is applied to the offshore test case of Middelgrunden, Denmark as well as to the onshore test case of Stag Holt – Coldham wind farm, UK. While aesthetic considerations have heavily influenced the famous curved design of the Middelgrunden wind farm, this work focuses on demonstrating a method that optimizes the profit of wind farms over their lifetime based on a balance of the energy production income, the electrical grid costs, the foundations cost, and the cost of wake turbulence induced fatigue degradation of different wind turbine components. A multi-fidelity concept is adapted, which uses cost function models of increasing complexity (and decreasing speed) to accelerate the convergence to an optimum solution. In the EU-FP6 TOPFARM project, three levels of complexity are considered. The first level uses a simple stationary wind farm wake model to estimate the Annual Energy Production (AEP), a foundations cost model depending on the water depth and an electrical grid cost function dictated by cable length. The second level calculates the AEP and adds a wake-induced fatigue degradation cost function on the basis of the interpolation in a database of simulations performed for various wind speeds and wake setups with the aero-elastic code HAWC2 and the dynamic wake meandering model. The third level, not considered in this present paper, includes directly the HAWC2 and the dynamic wake meandering model in the optimization loop in order to estimate both the fatigue costs and the AEP. The novelty of this work is the implementation of the multi-fidelity approach in the context of wind farm optimization, the inclusion of the fatigue degradation costs in the optimization framework, and its application on the optimal performance as seen through an economical perspective. Copyright © 2013 John Wiley & Sons, Ltd.

KEYWORDS

wind farm layout optimization; wind farm siting; dynamic wake meandering; foundation cost; optimization; wind farm wake; electrical grid cost

Correspondence

Pierre-Elouan Réthoré, Wind Energy Department, DTU, Risø Campus, DK-4000 Roskilde, Denmark.
E-mail: pire@dtu.dk

Received 17 June 2012; Revised 27 June 2013; Accepted 16 August 2013

NOMENCLATURE

(x_i, y_i)	The position of the ith turbine in a Cartesian grid
CT_g	Equals 2% of the total turbine cost
CT_r	Equals to 20% of the total turbine cost and refers to a reference water depth of 8 m, the gradient foundation cost per meter deviation from the reference water depth
$\Delta(x_i, y_i)$	The deviation of the water depth at location (x_i, y_i) from the reference water depth measured in meters
Γ	The cabling trace connecting all turbines in the shortest possible way
n_{WT}	The total number of turbines in the wind farm considered
C	The variable part of the total wind farm investment costs
$c(x, y)$	The cabling cost per running meter
D	Rotor diameter

D_{min}	The minimum distance between two turbines in the wind farm layout
D_S	The mean relative degradation of the particular component S
$F(D_S;\mu_{S,j};\sigma_{S,j})$	The log-Gaussian cumulative distribution function with distribution parameters $\mu_{S,j}$ and $\sigma_{S,j}$
$L_{d,S}$	The design equivalent fatigue load
$L_{\text{eq},S}$	The lifetime accumulated equivalent fatigue load
L_{eq}	Lifetime equivalent fatigue load
n_K	The number of possible locations
n_L	The number of times interests of the loans has to be paid times a year
N_R	A weight factor large enough to assure that more than $R_{\max}$ component replacements is unfavorable for the optimal wind farm topology
n_T	The number of 10−min cycles corresponding to 20-year lifetime ($6 \times 24 \times 365 \times 20$)
$n_{\text{eq},L}$	The lifetime equivalent number of cycles, set to 10^7 cycles
$p(U)$	The probability for the wind speed and wind direction
P_E	Price of electricity
P_S	The price of the particular component S
$P_{elec}(U)$	The electrical power at wind speed/wind direction case U
P_{Sr}	The replacement cost (i.e., cost of the physical component replacement and additional expenses originating from derived production loss)
R	Wind turbine rotor radius
$R_{\text{eq}}(U)$	The equivalent load for the load case U
$R_{\max}$	The maximum number of allowable replacements defined by the designer
S	The structural member considered
X	The wind farm life time in years
AEP	Annual energy production
CD	The accumulated components degradation (i.e., the cost of fatigue driven turbine degradation within this span of time)
CDF	Cumulative distribution function
CF	The costs of foundation
CG	The electrical infra structure costs (i.e., cables connecting the individual turbines to the wind farm transformer)
CM	The cost of overall maintenance
DWM	Dynamic wake meandering
FB	Financial balance
HAWC2	Horizontal axis windturbine code
O&M	Operation and maintenance
TEP	Total energy production
WP	The value of the wind farm power production over the wind farm lifetime
WP_n	The net value of the power production
WT_i	Wind turbine of index i
WTC	Wind turbine cost

1. INTRODUCTION

During recent years, wind energy has moved from an emerging technology to become a nearly competitive technology with conventional energy sources. An increased proportion of the turbines to be installed in the future, are foreseen to be sited in large wind farms. Establishment of large wind farms requires enormous investments, putting steadily greater emphasis on optimal topology layout. Today, the design of a wind farm is typically based on an optimization of the power output only, whereas the load aspect is treated in a rudimentary manner only, in the sense that the wind turbines are required only to comply with the design codes.

Wind farm layout optimization is a relatively new research topic, with some of the first articles on the subject includes Mosetti *et al*. in 1994[1] and Beyer *et al*. in 1996.[2] Since then, the topic has become gradually more popular to reach around 10 journal and conference articles produced every year (see[3] and[4] for a more exhaustive review). The vast majority of the research work on this topic has been focused on the types of optimization algorithm used to solve the problem, keeping the various cost functions as simple as possible. A notable exception to this observation is the work of Elkinton[5], which presents a rather sophisticated modeling of different costs function, in particular the electrical grid and foundation costs. While most consider the power losses because of wake effect, to the authors knowledge, none consider the costs associated

with the wake induced fatigue loads on the wind turbine components. However, a complete optimization of layout and control of wind farms requires, in addition to the power production, a detailed knowledge of the loading of the individual turbines. This is not a trivial problem. The power production and loading, related to turbines placed in a wind farm, deviate significantly from the production and loading pattern of a similar stand-alone wind turbine subjected to the same (external) wind climate.

To achieve the optimal economic output from a wind farm, an optimal balance between capital costs, operation and maintenance (O&M) costs, fatigue lifetime consumption of turbine components, and power production output is to be determined on a rational background. The overall objective of the TOPFARM project[6] is to establish this background in terms of advanced flow models that include instationary wake effects, advanced (and fast) aero-elastic models for load and production prediction as well as dedicated cost and control strategy models, and subsequently to synthesize these models into an optimization problem subjected to various kinds of constraints, as, for example, area constraints and turbine interspacing constraints. The design variables in the optimization problem are the relative position of the wind farm wind turbines (including the possibility for positioning a given number of turbines in one or more wind farms).

When considering a computationally demanding iterative process, it is of crucial importance, that the resulting models of the complex wind field within a wind farm can be condensed into fast, though accurate, flow simulation tools. The basic strategy for achieving this goal goes through a chain of flow models of various complexities, where the advanced and very demanding computational fluid dynamic (CFD) based models, together with available experimental evidence, are used to formulate, calibrate, and validate simpler models ranging from simplified CFD models to more engineering stochastic type of models.

Aero-elastic modeling is needed to calculate production as well as structural loads for each of the turbines in the wind farm. It is a challenge on one hand to keep computational costs limited, while on the other hand to have accurate prediction of the loads of each turbine. Complete aero-elastic calculations for each turbine are clearly not feasible due to the very large number of cases that need to be considered when taking into account wind direction and wind speed variations. In this work, a simplified approach is taken, where the fatigue load calculations are based on a database of precalculated generic load cases for turbines in wake operation. Aggregated lifetime equivalent loads can then be found by summing up contributions from the individual load cases.

When aiming at an economic optimization of wind farm topology, cost models are essential, encompassing both financial costs, and operating costs. Only costs that depend on the wind farm topology (including wind farm infra structure, wind turbine foundations, production, and loading) are relevant.[7] In the context of this work, these costs are denoted variable costs, contrary to fixed costs that are, for example, cost of planning and projecting of the wind farm, cost of the land available for the intended wind farm project, price of turbines (assuming a fixed number of turbines), and external civil engineering costs. The variable costs need to be evaluated only on a relative basis, whereas the knowledge of the absolute costs are not necessary for the optimization.

A proper optimization approach is essential for successfully carrying out the optimization. One aspect is the choice of the type of optimization algorithm among global methods and local gradient-based methods, where the likelihood of being captured in a local minimum needs to be traded off against rate of convergence and total computational costs. Another aspect is a clever mapping of the wind farm layout design variables by using as few variables as possible, thus limiting the feasible set, and how to include constraints on layout and on the wind farm performance characteristics (e.g., power fluctuations and space used). In order to speed up the optimization time, a multi-fidelity approach is proposed. Different types of multi-fidelity methods exist (see Robinson *et al.*[8] for a short review). The basic idea in this work is first to use a global optimization approach on the basis of simplified cost functions over a coarse discretization of the domain as well as the wind direction and wind speed distribution considered; and subsequently to refine the resulting layout by increasing gradually the complexity of the cost functions and the resolution of the discretization by using a gradient based optimization algorithm. The approach presented in this work is sequential, with the higher fidelity model being used to refine the result found by the lower fidelity model.

This paper presents a summary of activities leading to the implementation of the optimization methodology of the TOPFARM project. Further details and information can be found in a previous conference article[9] and in a technical report by the same authors of this article.[10]

The paper is structured as follows. The method section introduces the different optimization algorithms used in this work, the way they are constrained, and how they are setup using a multi-fidelity approach. The different cost functions are then presented followed by a description of the wind turbine aero-elastic and wake models they rely upon. Three test cases are presented in the result section: (i) a hypothetical six-turbine offshore wind farm, (ii) the existing Stags Holt–Coldham (UK) onshore wind farm consisting of 17 turbines, and (iii) the existing offshore wind farm of Middelgrunden (DK) consisting of 20 turbines. All cases give satisfying results and demonstrate the range of applications of the TOPFARM optimization platform. The discussion section presents different issues related to the implementation of the methods and running the test cases. Finally, in conclusion, it some future work ideas for improving the optimization framework is proposed.

2. METHOD

2.1. Multi-fidelity optimization

It is the purpose of the optimization tool to alter the wind farm layout so that the financial output over the wind farm lifetime is maximized. In the current work, the DTU Wind Energy in-house optimization platform, HAWTOPT, is used as the optimization engine[11–13]. HAWTOPT is a general purpose optimization tool with several different optimization algorithms included as options.

In the present optimization context, the so-called financial balance, which results from the involved cost functions, becomes the objective function, with the wind farm layout being described in terms of design variables. The constraints are then defined to limit the domain spanned by the design variables into a permissible region. Constraints may both be explicit limits on the individual wind turbine coordinates as well as integral values resulting from calculations in addition to the cost functions. These could be, for example, the maximum allowable turbine loads, minimum distance between turbines, power quality, and so on.

In the beta version of the tool, the optimization problem is defined within MATLAB, and during the optimization, MATLAB is acting as the working horse of the optimization. This means that a new design vector (i.e., wind farm layout) is generated by HAWTOPT and subsequently passed on to MATLAB. Matlab then calculates the objective function, which is returned to HAWTOPT. As the optimization process is iterative, a significant number of cost function evaluations are needed before the optimization is completed, resulting in an optimized wind farm layout.

2.2. Optimization algorithms

In this work, two optimizations algorithms of HAWTOPT are used: The sequential linear programming (SLP) method of Arora[14] and the simple genetic algorithm (SGA) of Goldberg.[15] The main reason for selecting these algorithm is that the authors had good experience working with them for wind turbine rotor optimization in previous works.

2.2.1. Sequential linear programming.

The SLP method is a linear algorithm within a linear subspace of the feasible set. Move-limits are applied in all dimensions to ensure smooth convergence. The move-limits are adaptive and automatically adjusted according to the convergence toward an optimum on basis of the rate of convergence.[14] The SLP approach typically has an attractive rate of convergence and is therefore efficient in terms of the number of cost function evaluations required. However, this is at the expense of being sensitive to local minima. In a nonlinear feasible set, there is no guarantee to reach at the global optimum.

2.2.2. Simple genetic algorithm.

The SGA is a genetic algorithm based on the original work of Goldberg.[15] in which the design variables are mapped on chromosomes (binary strings). By using an analogy to the theory of evolution, individual parents mate and create children by use of genetic operators, crossover, and mutation. Automatic fitness scaling is used, and constraints are included by a penalty formulation.[16] In our experince, we found that the SGA approach has a much slower rate of convergence compared with the SLP approach. However the advantage of the SGA method is that if run for an infinite number of iterations, it is more likely going to converge to the global optimum than SLP, which tends to converge to local minimum. In practice, however, the SGA method is not expected to find the global optimum as it is run for a limited amount of iterations, until it seems to have converged to a solution.

The combination of the SGA and SLP approaches is appealing, if the SGA method is used for an initial optimization using a coarse resolution of the design variable, and subsequently when an optimum is reached, the gradient based SLP method can be used subsequently to refine the result using a finer resolution of the design variables. In this way, the global optimality advantage of the SGA is combined with the accuracy of SLP. Note that this way of combining SGA and SLP has comparable non-local optimization features to a multi-start SLP optimization.

2.3. Wind farm layout concepts

Keeping the number of design variables as low as possible is the key to keep the computational costs at a minimum, because more design variables slow down convergence and requires more objective function evaluations.

Two different approaches for mapping the wind farm layout into design variables are used in this work. The first uses the unstructured turbine x and y position cartesian coordinates directly as design variables, thus resulting in two design variables for every turbine.

The second uses a transformation of the wind farm (x,y) domain into a single parameter. A grid of possible locations within the domain is mapped, with each point of the grid accessible through an index number. This has the additional advantage that turbines cannot end up outside of the permissible domain, and consequently it is not necessary to define

Table I. Schematic representation of the multi-fidelity optimization approach.

Fidelity Level	First	Second	Third
Energy production	HAWC2-DWM database	HAWC2-DWM database	HAWC2-DWM simulations
Fatigue costs	HAWC2-DWM database	HAWC2-DWM database	HAWC2-DWM simulations
Foundation costs	Yes	Yes	Yes
Electrical Grid costs	Yes	Yes	Yes
Optimization algorithm	SGA	SLP	SLP
Domain discretization	Coarse	Fine	Fine
Wind speed and direction bin size	Coarse	Fine	Fine

DWM, dynamic wake meandering; SGA, simple genetic algorithm; SLP, sequential linear programming.

constraints to ensure that turbines satisfy possible area constraints. Especially the SGA method and other native unconstrained methods will benefit from this type of mapping by avoiding the use of a penalty function for constraint implementation.

In this work, the first mapping is used with the SLP algorithm, and the second mapping is used with the SGA algorithm.

2.4. Multi-fidelity approach

In order to speed up the convergence of the optimization, the TOPFARM platform proposes to use a multi-fidelity approach. The idea is to carry out the largest part of the optimization by using simpler/faster cost functions combined with coarse resolution and subsequently to refine progressively the results by increasing the resolution of the design domain and the complexity of the models. Three levels of increasing complexity and precision are proposed (see Table I). However, this work focuses only on the first two levels of the multi-fidelity optimization approach. The third level is indicated here only as a logical extension of this multi-fidelity approach and will be considered in a future work. In this work, the main difference between level 1 and level 2 is the type of optimization algorithm (i.e., SGA for level 1, and SLP for level 2): the domain mapping and the wind speed/direction bin sizes.

2.5. Position constraints

Two types of position constraints are enforced in this work: (i) the wind turbine absolute position must be inside the boundaries of a region, and (ii) the spacing between any turbines in the farm must not be less than one rotor diameter. These constraints are enforced differently for the SGA and the SLP methods, respectively.

2.5.1. Domain boundaries.

Some external factors can limit the admissible locations of the wind farm, and it is thus necessary to be able to restrain the possible positions of the wind turbines to a feasible domain. In this work, the boundaries of the domain are defined by a polygon. Depending on how the design variables are defined, the boundaries of the domain are enforced differently. The SLP algorithm uses unstructured design variables for each direction of the possible turbine coordinates. To restrain the locations of the turbines, a norm of the distance between each turbine and the domain boundaries is calculated. If all wind turbines are within the domain, then the norm becomes the distance from the boundary to the closest wind turbine. If one or more wind turbines are outside the boundaries, the norm sums the negative distance between the boundary and the outlying wind turbines. A constraint is then put on this norm, enforcing the optimization algorithm to ensure that it is positive.

The SGA is, however, not very efficient with constraints, because they need to be added as a penalty to the objective function. Therefore, a more efficient method is to use a more clever design variable mapping, which limits the possible layout candidates by defining the design variables as an index on a list of fixed points located inside the boundaries of the domain (Figure 1).

The advantage of this approach is that the wind turbine positions are automatically bounded inside the polygon domain. Therefore there is no need to define a constraint on the wind turbine position. Furthermore it is possible to control the spacing between the possible locations, and consequently limit the number of possible wind farm layout n_F to

$$n_F = \prod_{i=1}^{n_{\mathrm{WT}}} n_K - i \tag{1}$$

where n_{WT} is the number of turbines and n_K the number of possible locations. The spatial resolution of the grid is therefore directly linked to the speed of convergence of the genetic algorithm. Moreover, this approach gives a number of design variables equal to the number of turbines, which is thus reduced by a factor two, compared to a discretization of the domain in two coordinates, as done with the SLP algorithm, which will further speed up the convergence.

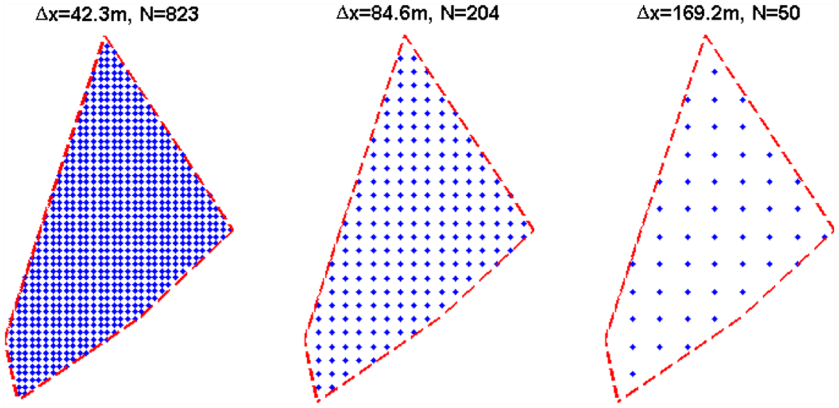

Figure 1. Discretization of the domain with different spacing.

2.5.2. Minimum distance between wind turbines.

There is a physical minimum distance, under which two wind turbines are too close to each other to operate under normal conditions. For instance, two turbines next to each other can obviously not operate, if they are located at a mutual distance lower than one rotor diameter from each other. Therefore, there is a need to enforce this constraint to avoid unrealistic solutions. However, the two different optimization approaches handle this constraint differently.

The approach used for the gradient-based SLP is based on the definition of a norm quantifying the distance between each turbine and its closest neighboring turbine. Similarly to the domain boundary norm, this norm is positive when the minimum distance between turbines is larger than the minimum allowable distance. In this work, the minimum distance ($D_{\min}$) is set to one rotor diameter (1D). In this case, the norm returns the minimum distance between two turbines in the wind farm layout. In the case where two or more wind turbines are violating this constraint, the norm returns the negative sum of all the residual distances between turbines that fail to meet the criteria. The mathematical expression of the norm is given as follows (equation 2):

$$\text{Norm} = \begin{cases} \min_{i,j} \left[\text{dist}(\text{WT}_i, \text{WT}_j)\right], \text{when no turbine fail} \\ \sum \text{dist}(\text{WT}_i, \text{WT}_j) - D_{\min}, \forall (i,j) \in \{\text{Failing Turbines}\} \end{cases} \tag{2}$$

where $D_{\min}$ is the minimum acceptable distance between two turbines in the wind farm layout and WT_i denotes the ith wind turbine.

Standards require the wind turbines to be located at larger mutual distances than two rotor diameters. This requirement is based on considerations related to wake deficits and added turbulence, which might harm downwind turbines. These effects are implicitly taken into account in the wake models. The minimum distance requirement is here only taking care of the special case, where wind turbines are unable to operate because of possible blade contact between two turbines.

Because our implementation of the SGA is not performing well with constraints, a different approach is taken. The chosen mapping by itself ensures that turbines cannot be located at a closer distance than one rotor diameter, except for the case where the turbines are located exactly on top of each other. In this special case, it is assumed that one of the wind turbines is not operating. However, all the other costs are assumed unchanged. This has essentially the same effect as a penalty function but with the scaling of the penalty directly on amounts included in the financial balance.

2.6. Cost functions

In an optimization context, the synthesis of all required submodels is performed by formulating an objective function. In the framework of TOPFARM this objective function is formulated in economical terms, as a logical consequence of TOPFARM aiming at an overall economic optimization of the wind farm topology. The need of cost models for all costs depending on the wind farm topology arises.

The cost modeling is built upon two governing principles: relevance and relative cost basis. Only costs that are relevant to the topology optimization problem are included in the objective function, in contrast to costs that are irrelevant. Furthermore, costs are evaluated on a relative cost basis. The optimization seeks to find the optimum wind farm layout applying mathematical concepts, which compare the actual wind farm topology with alternatives and thereby only needs the relative difference in cost for these different alternatives. It is therefore not necessary to model the total absolute costs. However,

the relative impact of involved costs must be correct. We will denote such costs as variable costs, and in the following present a simplified version of the cost modeling described in the work of Larsen.[7]

2.6.1. Financial balance.

Based on two financial parameters – all referring to a 1-year period – the rate of inflation, r_i and the interest rate that the wind farm consortium has to pay for loans (i.e., price of money in banks or by other investors), r_c, the objective function is formulated as the following financial balance in the work of Larsen,[7] (equation 3)

$$\mathrm{FB} = \mathrm{WP}_n - C\left(1 + \left(\frac{r_c - r_i}{n_L}\right)\right)^{Xn_L} \tag{3}$$

in which WP_n denotes the net value of the power production, C denotes the variable part of the total wind farm investment costs, n_L is the number of times interests of loans has to be paid a year, and X is the design wind farm life time in years. The net value of the power production is here defined as

$$\mathrm{WP}_n = \mathrm{WP} - \mathrm{CD} - \mathrm{CM} \tag{4}$$

where WP is the value of the wind farm power production over the wind farm lifetime, CD is the accumulated cost of components degradation (i.e., the cost of fatigue driven turbine degradation within this span of time), and CM is the cost of overall maintenance. The financial costs is in turn defined as

$$C = \mathrm{CF} + \mathrm{CG} \tag{5}$$

with CF being the costs of foundation and CG being electrical infra structure costs (i.e., cables connecting the individual turbines to the wind farm transformer).

2.6.2. Foundation costs.

The foundation costs are assumed as

$$\mathrm{CF} = \sum_{i=0}^{n_{\mathrm{WT}}} \mathrm{CT}_i(x_i, y_i) \tag{6}$$

where CT_i is the cost of foundation for the ith wind turbine, (x_i, y_i) is the position of the ith turbine in a Cartesian grid, and n_{WT} is the total number of turbines in the wind farm considered. The cost of foundation, thus, in general depends of the individual location of the turbines and thereby in turn on the wind farm topology. Without a more detailed description of the foundation technology and costs, we propose to define a very simple definition of the wind turbine foundation cost, only based on the water depth. For the water depths relevant for the demonstration offshore case we will more specifically assume that CT_i depends linearly with the water depth as

$$\mathrm{CT}_i(x_i, y_i) = \mathrm{CT}_r + \Delta h(x_i, y_i)\mathrm{CT}_g \tag{7}$$

where the reference foundation cost CT_r equals 20% of the total turbine cost and refers to a reference water depth of 8m, the gradient foundation cost per meter deviation from the reference water depth, CT_g, equals 2% of the total turbine cost, and $\Delta h(x_i, y_i)$ is the water depth at location (x_i, y_i) minus the reference water depth measured in meters.

2.6.3. Electrical costs.

The cost of the electrical infrastructure is modeled as

$$\mathrm{CG} = \int_{\Gamma} c(x, y)ds \tag{8}$$

where $c(x, y)$ is the cabling cost per running meter, Γ is the cabling trace connecting all turbines in the shortest possible way, and ds is an infinitesimal curve element on the trace. Note, that for a more detailed modeling, the best strategy is not necessary to base the cabling on the shortest possible cabling but rather on the cheapest possible cabling. This is elaborated on in more detail by Larsen,[7] where such a formulation is derived.

The idealized cables used in this analysis are assumed to be able to carry all the electricity of the wind turbines connected through them. However, this simplified approach may have an impact on the optimization process and the final optimal solution, and should therefore be considered in future work.

In the current implementation, the cabling layout is defined using a deterministic clustering algorithm. The algorithm can be decomposed in two phases (Figure 2).

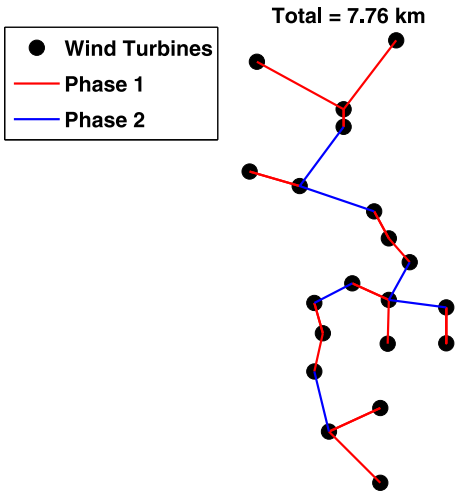

Figure 2. Grid clustering algorithm.

Table II. Assumed prices for cable costs per running meter.

In € / m	Offshore	Onshore
Cable	270	135
Installation	405	135
Total	675	270

In the first phase, each wind turbine is connected to its closest neighbor. This generates several groups of interconnected wind turbines. In the second phase, each group of turbine is connected with its closest neighboring group, through their closest elements. This phase is successively carried out, until all the wind turbines are connected together through the layout.

The cable costs used in this work are assumed to be independent of the sea bed soil type and water depth. Without access to more realistic prices, the combined cable, and cable installation costs are estimated through an 'educated' guess and given in Table II.

2.6.4. Fatigue degradation and operation and maintenance costs.

Fatigue degradation is a stochastic process driven by stochastic loading of the turbines. The fatigue degradation of the turbines is accounted for in this work by linear depreciation of the component value. For a particular structural member, identified by S, the mean cost of fatigue load degradation is presumed proportional to the mean accumulated equivalent fatigue load, associated with a suitable component hot spot, caused by turbine operation during the lifetime of the wind farm. We introduce the mean relative degradation of the component S as D_S (equation 9)

$$D_S = \frac{L_{\mathrm{eq},S}}{L_{d,S}} \tag{9}$$

with subscript S referring to the structural member considered, and where $L_{\mathrm{eq},S}$ and $L_{d,S}$ are the lifetime accumulated and the design equivalent fatigue loads, respectively. By using equation (9), the cost of degradation, CD_S, is defined as

$$\mathrm{CD}_S = P_S D_S \tag{10}$$

with P_S denoting the price of the particular structural component.

In the formulation of operation and maintenance (O&M) costs we apply a probabilistic failure criterion. Assuming the component equivalent fatigue loads to be described by a log-Gaussian distribution,[17] the cost of maintenance, CM_S, related to the structural member S, is approximated as[7]

$$\mathrm{CM}_S = N_R P_{Sr} F\left(D_S; \mu_{S,(R_{\max}+1)}, \sigma_{S,(R_{\max}+1)}\right) + P_{Sr} \sum_{j=1}^{R_{\max}} F\left(D_s; \mu_{S,j}, \sigma_{S,j}\right) \tag{11}$$

where P_{Sr} denotes the replacement cost (i.e., cost of the physical component replacement and additional expenses originating from derived production loss), $R_{\max}$ is the maximum number of allowable component replacements defined by the designer, and N_R is a weight factor large enough to assure that more than $R_{\max}$ component replacements is unfavorable for the optimal wind farm topology. $F(D_S; \mu_{S,j}, \sigma_{S,j})$ is the log-Gaussian CDF with distribution parameters $\mu_{S,j}$, and $\sigma_{S,j}$. The jth distribution parameter set is related to the mean lifetime equivalent fatigue load, $E[L_{\text{eq},S}]$, and variance of the component equivalent fatigue load, $\text{VAR}[L_{\text{eq},S}]$, through the respective mean and variance of the relative degradation measured as[7]

$$\sigma_{S,j} = \sqrt{\ln\left(\frac{\text{VAR}[L_{Sr}]}{j^2 L_{d,S}^2} + 1\right)} \tag{12}$$

and

$$\mu_{S,j} = \ln(j) - \sigma_{S,j}^2 \tag{13}$$

The costs of degradation, described in equation (10), and the costs of maintenance, described in equation (11), are straight forwardly generalized to all main components on all turbines within the considered wind farm as

$$\text{CD} = \sum_{N_T} \sum_{S} P_S D_S \tag{14}$$

and

$$\text{CM} = \sum_{N_T} \sum_{S} \text{CM}_S \tag{15}$$

respectively.

In this work, the design equivalent fatigue load, $L_{d,S}$, is defined in percent of the lifetime accumulated equivalent fatigue load, $L_{\text{eq},S}$, of a hypothetical isolated wind turbine (i.e., without wind farm wake effect). For this reason, some components, like the gearbox and the generator, which normally scale with the power output and would therefore have, under the current assumptions, a lower fatigue than an isolated turbine, are here assumed to be part of the nacelle components.

The prices used for calculating degradation as well as O&M costs are given in Table III.

2.6.5. Energy production sales.

The total energy production (TEP) is calculated by summing up the wind farm power contributions from the different wind speeds and wind directions taking into account the probability of each set of wind speed and wind direction:

$$\text{TEP} = \sum_{j=1}^{n_{WD}} \sum_{i=1}^{n_{WS}} P_{\text{elec}}(U_{i,j}) p(U_{i,j}) n_T \tag{16}$$

where $P_{\text{elec}}(U_{i,j})$ is the electrical power at wind speed/wind direction case $U_{i,j}$, n_T is the number of 10-min sequences corresponding to a 20-year lifetime (6×24 h $\times$ 365 days $\times$ 20 years), and $p(U_{i,j})$ is the probability for the particular wind speed (with index i) and (wind direction with index j). The price of electricity is defined in this work as $P_E = 50$ € /MWh. The total value of the wind farm power production is therefore defined as

$$\text{WP} = P_E \text{TEP} \tag{17}$$

Table III. Components and replacement costs for the wind turbine used in this paper as well as cost drivers.

Turbine component	Degradation P_S relative to turbine cost (%)	Replacement P_{Sr} relative to turbine cost (%)	Design loads $L_{d,S}$ relative to isolated turbine L_{eq}, S (%)	Cost driver
Rotor	20	25	250	Blade root flapwise moment
Nacelle components	10	30	250	Tower top tilt moment
Gearbox and generator	20	30	250	Electrical power
Tower	20	50	250	Tower base bending moment
Fixed part	30			

2.7. Wake models

Two wake models have been developed for this work: a detailed instationary wake model and a faster stationary wake model. The instationary DWM model,[18–23] combined with the aero-elastic wind turbine simulation tool HAWC2,[24] is used to estimate the 10-min averaged power production and equivalent fatigue of various wind turbine components under various inflow wake conditions . The stationary model[19] is used to estimate the normative mean wind speed at the position of each wind turbine in the wind farm ('normative' is defined here as the equivalent undisturbed free-stream wind speed that the wind turbine would be operating under to produce a similar induced velocity at the rotor position). This wind speed is used to estimate the lifetime fatigue and the annual energy production of each wind turbines (based on a HAWC2–DWM database at the second level and on direct HAWC2–DWM simulations at the third level). These two models are described in further details in the following two subsections.

2.7.1. Instationary model.

The downstream advection of a wake emitted from an upstream turbine describes a stochastic pattern known as wake meandering.[21,25] It appears as an intermittent phenomenon, where winds at downwind positions may be undisturbed for part of the time but interrupted by episodes of intense turbulence and reduced mean velocity as the wake hits the observation point.

To deal with this problem the DWM model[18,21,22,26] was used. The DWM model describes the essential physics of the problem, and accounts for both the observed increased turbulence intensity of wake flow fields and the modified turbulence structure.

The basic philosophy of the DWM model is a split of scales in the wake flow field, based on the conjecture that large turbulent eddies are responsible for stochastic wake meandering only, whereas small turbulent eddies are responsible for wake attenuation and expansion in the meandering frame of reference as caused by turbulent mixing. It is consequently assumed, that the transport of wakes in the atmospheric boundary layer can be modeled by considering the wakes to act as passive tracers driven by a combination of large-scale turbulence structures and a mean advection velocity, adopting the Taylor hypotheses. The DWM model is essentially composed of three corner stones: (i) a model of the wake deficit as formulated in the meandering frame of reference, (ii) a stochastic model of the downstream wake meandering process, and (iii) a model of the self induced wake turbulence described in the meandering frame of reference. Detailed descriptions of the various submodels and their implementation in the framework of the aero-elastic code HAWC2 can be found in the following references.[20–22,24]

2.7.2. Stationary model.

A stationary wake model for wind farm flow modeling has been developed for the TOPFARM platform.[19] It uses the wind turbine thrust coefficient curve and the ambient atmospheric turbulence intensity upstream of the wind farm to estimate the deficit of an assumed axis-symmetric single wake. The estimation of the individual wake contributions are based on a closed form asymptotic solution to the thin shear layer approximation of the NS equations, assuming rotational symmetric flow conditions.

The expansion of stationary wake fields is believed to be significantly affected by meandering of wake deficits as, for example, described by the DWM model. In the present model, this effect is approximately accounted for by imposing suitable empirical downstream boundary conditions on the closed form formulation of the wake expansion, these depend on the rotor thrust and the ambient turbulence conditions, respectively. For downstream distances beyond approximately 10 rotor diameters (at which distance the calibrated wake expansion boundary conditions are imposed), the present formulation of wake expansion is, however, believed to underestimate wake expansion.

In order to account for multiple wakes, all the upstream single wake deficits are combined using a linear summation. In order to estimate the equivalent undisturbed inflow wind speed at a wind turbine, the model performs a Gauss integration over the rotor area of the undisturbed inflow wind profile combined with the upstream generated wake deficits.

2.8. Wake induced loads database

The cost of components degradation as well as the O&M costs take as inputs the lifetime equivalent fatigue loads of different wind turbine components (L_{eq}). These fatigue loads are calculated using aero-elastic simulations of all wind turbines at all possible ambient wind speeds and wind directions. The complexity of this task can be dramatically reduced under the assumption that only the closest turbine is contributing significantly to the inflow wake effect for a particular wind direction. Under this assumption, it is possible to build a database of generic load cases defined in terms of parameters such as the inflow wind speed, the ambient turbulence intensity, the distance from the upstream wind turbine, and the angle between a vector connecting the location of the two wind turbines and a wind direction vector. Such a database needs a large amount of simulations to cover all the relevant wake cases.

Table IV. HAWC2 sensors for load analysis.

Sensor	Wöhler exponent
Tower base over turning bending moment	4
Nacelle (tower top) tilt moment	8
Blade root flapwise bending moment	12
Electrical power	—

In the present work, 7500 simulations (covering wind speeds from 4 to 26 m/s with a step of 2 m/s; inflow turbulences of 1%, 5%, 10%, and 15%; 13 azimuth angles from 0 to 45 °; distance from upstream turbine from 1D to 20D) each of 600 s were computed on DTU cluster by using the aero-elastic code, HAWC2[27] combined with the DWM model described in the previous section. To improve the statistical significance, each type of simulation is performed using the Mann turbulence model with six different seeds to generate the inflow wind turbulence. The turbine used to generate the database is the 5MW reference turbine from the EU-project, UpWind. The data describing this fictitious turbine was designed by National Renewable Energy Laboratory.[28] Required estimates are obtained from the database with a 4D linear interpolation to estimate the cases falling in-between the computed cases.

The load analysis involves computation of statistical information as well as of fatigue load estimation on the basis of rainflow counting using Wöhler curve m-exponents representative for the respective component materials. Rainflow counting is performed using a standard Rainflow counting routine,[29] and a subsequent Palmgren-Miner approach is used to quantify the fatigue loads. The sensors listed in Table IV are defined for the load analysis. In addition to the three load sensors, the electrical power is included in the statistical analysis to enable the estimation of the AEP.

For each load sensor, the Rainflow counting results in an equivalent load, R_{eq}, defined as

$$R_{\text{eq}} = \left(\frac{\sum n_i R_i^m}{n_{\text{eq}}} \right) \tag{18}$$

where $\sum n_i R_i^m$ is the lifetime damage accumulation as based on the actual time series, and n_{eq} is the number of 600-s cycles during 20 years.

2.9. Lifetime equivalent fatigue loads

The lifetime equivalent fatigue load can be calculated by summation of contributions from all individual load cases taking into account the probability of each load case and the total number of equivalent cycles

$$L_{\text{eq}} = \left[\frac{1}{n_{\text{eq},L}} \int R_{\text{eq}}(U)^m n_{\text{eq}} p(U) n_T \, dU \right]^{\frac{1}{m}} \tag{19}$$

where $R_{\text{eq}}(U)$ is the equivalent load for the load case, defined by the mean wind speed U, n_{eq} is the number of 600 s cycles corresponding to $R_{\text{eq}}(U)$. $p(U)$ is the probability for the load case equal to the number of operation hours in the 20-year lifetime divided by number of hours in 20 years, n_T is the number of 10-min cycles corresponding to a 20-year lifetime ($6 \times 24 \times 365 \times 20$), and $n_{\text{eq},L}$ is the lifetime equivalent number of cycles, set to 10^7 cycles.

For the fatigue load cases, which appear from normal operation at different wind speeds and different wind directions, the probability is determined from the wind rose, which defines the number of hours for each mean wind speed sector and the mean wind direction sector. This means that the summation for L_{eq} is carried out for all mean wind speeds in each mean wind direction sector, resulting in a total number of contributions as the product of the number of wind rose divisions, n_{WD}, and the number of mean wind speeds, n_{WS}

$$L_{\text{eq}} = \left[\frac{1}{n_{\text{eq},L}} \sum_{j=1}^{n_{\text{WD}}} \sum_{i=1}^{n_{\text{WS}}} R_{\text{eq}}(U_{i,j})^m n_{\text{eq}} p(U_{i,j}) n_T \right]^{\frac{1}{m}} \tag{20}$$

The lifetime equivalent fatigue loads computed according to equation (20) can then directly be used in equation (9).

2.9.1. Scaling of loads to different turbine sizes.

The database shall ideally be determined on the basis of load calculations for the specific turbine in question. If this is not possible, this section describes a first order approach, not necessarily conservative, to adapt the current load set to a different turbine size.[6] The scaling of loads is only valid for turbines having a similar power and load control. Moreover, it is restricted to turbines that are geometrically similar and of same concept as the turbines used to determine the current load set. The scaling is simplified to depend on the rotor radius, R, only. The tower only takes into consideration the aerodynamic loads, and it is assumed that the rotor load scales with R^2, while the moment arm scales with R, when assuming that tower height scales with R for geometrically alike turbines. This makes the static tower moment to scale with R^3. It is here assumed that the fatigue lifetime equivalent loads scale likewise. The flapwise moment and the aerodynamic load scales with R^2. The edgewise blade moments scale with R^4. The blade chord, and obviously also the blade length, scale with R. The static aerodynamic flapwise moment scale with R^3. As for the tower, we assume that the fatigue lifetime equivalent load scales with R^3. The rotor power scales with the nominal power of the turbine.

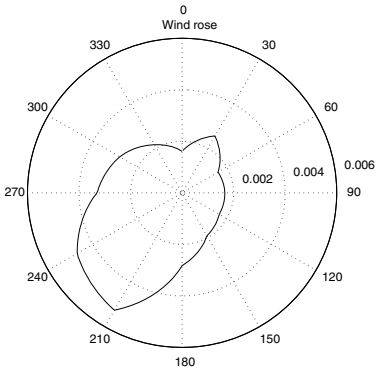

(a) Wind rose: probability of occurrence of wind direction (-).

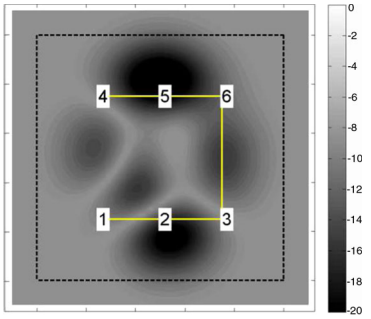

(b) Baseline layout. The color scale indicates the water depth in meters.

Figure 3. The 2 × 3 fictitious wind farm test case.

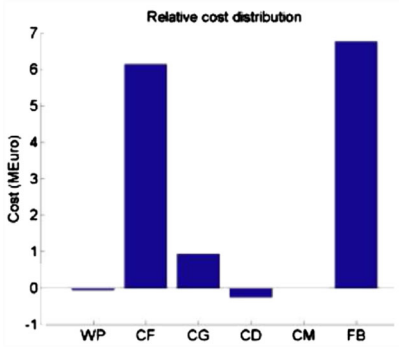

(a) Relative cost compared with the baseline layout. WP: Electrical sales, CF: Foundations costs, CG: Electrical grid costs, CD: Degradation costs, CM: Maintenance costs, FB: Financial balance. Positive means that it increases the financial balance of the wind farm.

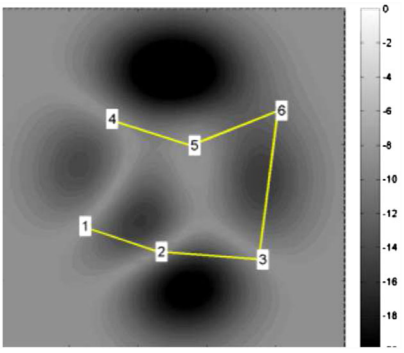

(b) Layout optimization result. The color scale indicates the water depth in meters.

Figure 4. Results of the sequential linear programming optimization of the 2 × 3 fictitious test case.

3. RESULTS

This section presents three wind farm cases to test and to demonstrate the capabilities of the models presented. These test cases are to be considered as proof of concept, as the real prices of the different elements of the financial balance were in large part unknown for the authors. The first test case is a hypothetical offshore wind farm. The second test case is the onshore wind farm at Stags Holt–Coldham, in UK. The third test case is the offshore wind farm of Middelgrunden, in Denmark.

3.1. 2 x 3 fictitious wind farm test case

A simple test case is designed and subsequently used to validate the method. Its a hypothetical offshore wind farm consists of 6 5MW turbines located on an area, where the water depth varies from 4 to 20 m. The wind climate at this location, the water depth, and the baseline layout are illustrated in Figure 3(b).

A first simulation is carried out using only the SLP optimization algorithm (equivalent to a level 2 optimization) by using the baseline layout presented in Figure 3(b). Figure 4 shows the optimization result and the relative change in the

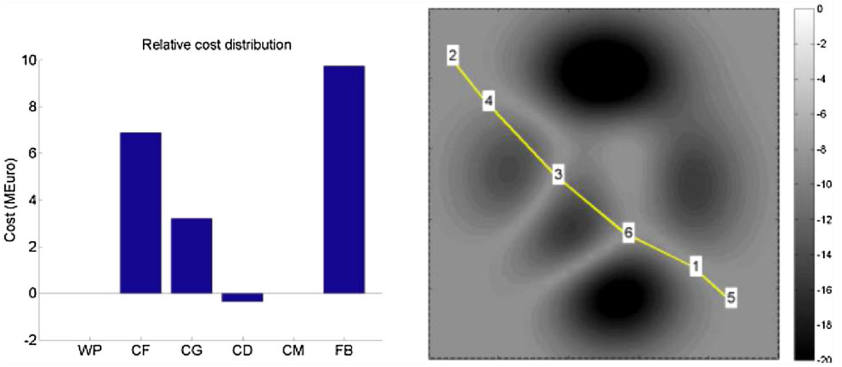

(a) Relative cost compared with the baseline layout. WP: Electrical sales, CF: Foundations costs, CG: Electrical grid costs, CD: Degradation costs, CM: Maintenance costs, FB: Financial balance. Positive means that it increases the financial balance of the wind farm.

(b) Layout optimization result. The color scale indicates the water depth in meters.

Figure 5. Results of the simple genetic algorithm+sequential linear programming optimization of the 2 × 3 fictitious test case.

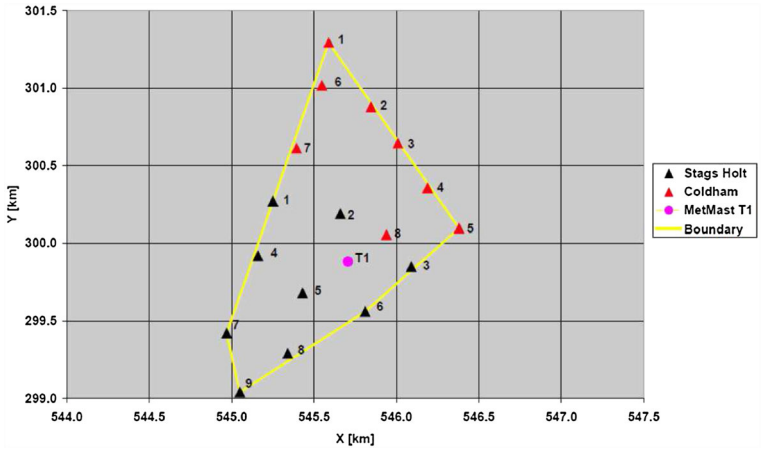

Figure 6. Stags Holt/Coldham baseline layout and allowed area for wind turbine locations.[30]

cost functions compared with the baseline layout. The results show a saving of 6.7M€ which is equivalent to 1.34 wind turbine cost (WTC) in comparison with the reference layout. Most of the savings have been found on the foundations costs, with the wind turbine being positioned on more shallow water locations in the optimized solution compared with the baseline layout.

A subsequent simulation by using an SGA+SLP approach (corresponding to level 1 + 2 of the multi-fidelity approach) is also presented. Figure 5(b) shows the optimized wind farm layout. The resulting wind farm layout is very close to be a straight line oriented perpendicular to the dominant wind direction, where the individual turbines are nicely placed at the lowest possible water depths. Figure 5(a) shows the change in the different financial balance elements. The overall improvement in the financial balance is 9.7 M€ (1.94 WTC). It can be seen that mainly the cost reductions for foundation and electrical grid layout caused the improvement, whereas energy production and turbine degradation are nearly unaffected.

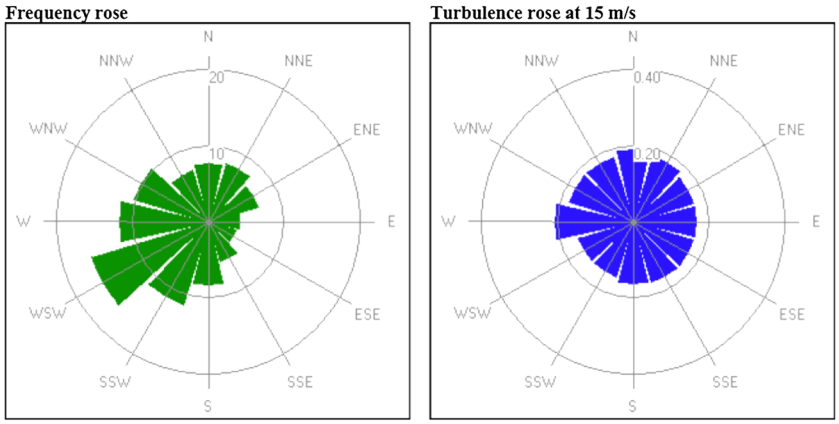

Figure 7. Stags Holt/Coldham wind rose (%) and turbulence rose.[30]

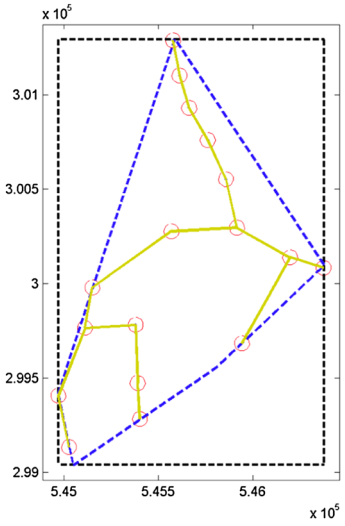

(a) Optimum wind farm layout.

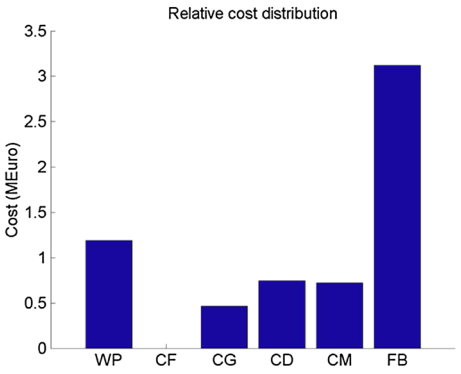

(b) Relative cost compared with the baseline layout.. WP: Electrical sales, CF: Foundations costs, CG: Electrical grid costs, CD: Degradation costs, CM: Maintenance costs, FB: Financial balance. Positive means that it increases the financial balance of the wind farm.

Figure 8. Results of the Stags Holt / Coldham test case using the simple genetic algorithm+sequential linear programming algorithm.

A simulation by using a pure SGA is also carried out (corresponding to level 1 of the multi-fidelity approach). Its results are very close to the SGA+SLP. The results are not shown here but are available in the works of Larsen *et al*. and Réthoré *et al*.[6,10] In this specific test case, the SLP refinement has very little improvement in comparison with the level 1-SGA approach.

3.2. Stags Holt/Coldham test case

The Stags Holt–Coldham wind farm is in reality two integrated onshore wind farms that in total is composed of 17 Vestas V80 wind turbines with 80-m rotor diameter and 60-m hub height. The wind farm is located on a flat and homogeneous terrain in between March and Wisbech in Cambridgeshire, UK. Foundation costs are thus not variable and are therefore not relevant for the optimization. These are consequently omitted from the objective function (i.e., the financial balance). The baseline layout and the boundary enclosing the area restriction of the optimization are shown in Figure 6.

Detailed information about the wind climate of Stags Holt/Coldham can be found in an technical report.[30] The wind rose and the turbulence intensity distribution are illustrated in Figure 7.

The first level of optimization ran SGA for 1000 iterations, and subsequently the second level ran SLP for 30 more iterations. Further iterations could not improve the financial balance. The initial SGA run resulted in an improvement of the financial balance of 1.5 M€ (0.75 WTC) and the subsequent SLP warm start resulted in a total improvement of the financial balance of 3.1 M€ (1.55 WTC) compared with the baseline.

Figure 8(a) shows the resulting wind farm layout after the SGA+SLP optimization. The solution is not fundamentally different from the baseline layout. The turbines are, however, not as regularly laid out, but rather on different connecting strings that seems to utilize the electrical grid costs better and even allow for improving the energy production. The change in financial balance and its subcomponents in Figure 8(b) shows that the total improvement of the financial balance is contributed to by all elements including turbine degradation and O&M.

3.3. Middelgrunden test case

The second test case considered is the offshore wind farm Middelgrunden, located at a close distance from the coast of Copenhagen, Denmark. It is composed of 20 Bonus B80 2MW wind turbines with a rotor diameter of 76 m and a hub

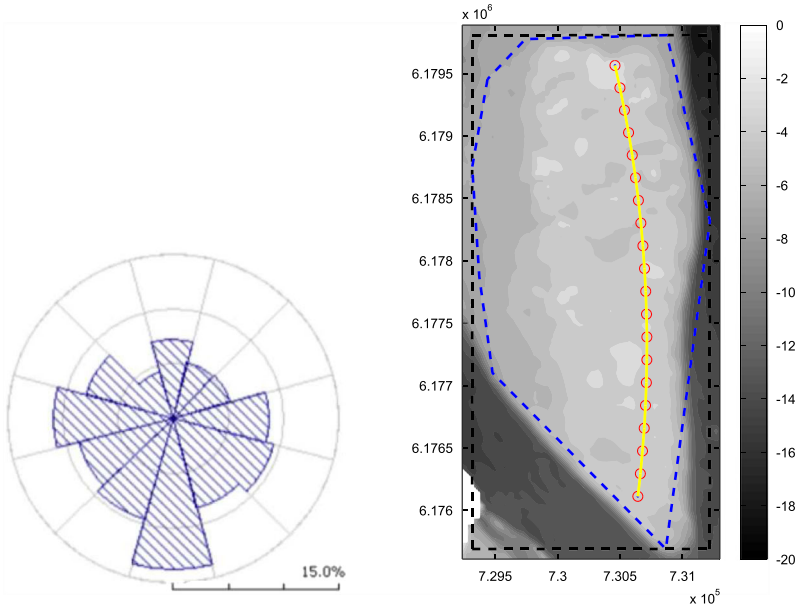

(a) Wind rose: probability of occurrence of wind direction (%).

(b) Existing wind farm layout. The color scale indicates the water depth in meters.

Figure 9. Middelgrunden test case.

height of 64 m. The wind climate of Middelgrunden is described in details in a technical report[31] and is summarized in Figure 9(a).

The wind turbines are arranged in a beautiful arc with a 2.3D turbine spacing (Figure 9(b)). The wind farm is located on an area relatively elevated compared with the averaged surrounding water depth of this location. The delimitation of the wind turbine allowed positions are following closely the border of the elevated area of this site (Figure 9(b)).

The first level of optimization ran SGA for 1000 iterations and subsequently the second level ran SLP for 20 more iterations. Further iterations could not improve the financial balance. The initial SGA-based optimization resulted in an improvement of the financial balance of 0.6 M€ (0.3 WTC) and the subsequent SLP warm start resulted in a total improvement of the financial balance of 2.1 M€ (1.05 WTC) compared with the baseline.

Figure 10 shows the optimized wind farm layout and the associated improved financial balance as compared with the baseline layout.

Figure 11 presents in details the costs associated with each turbine normalized with the value of the energy production of the same turbine. So if the total bar would reach 1, the costs associated with that turbine equals the value of the energy production by the turbine.

The wind turbine number and the contour distribution of the electrical power production and of the tower base flange moment are illustrated in Figure 12. This figures illustrate how the electrical production and tower moment are distributed geographically within the park. It can give a qualitative idea of how the wind turbines interact in the wind farm.

4. DISCUSSIONS

The results from the 2×3 fictitious test case show, that both the SLP and the SGA algorithms arrive at an optimum solution and that the financial balance can be improved over the baseline layout. It is clear that the SLP case in Figure 4 arrived at a local optimum. The initial baseline layout is still recognizable and the improvement of the financial balance is only 6.7 M€ (1.34 WTC) compared with the SGA result of 9.7 M€ (1.94 WTC). On the other hand the SGA result (with SLP refinement) in Figure 5 shows no resemblance with the initial baseline layout. It should be noted, that the total computational costs for the SGA case were approximately six times higher than for the SLP case. It appears, that the combination of a global SGA approach with a local SLP refinement works well taking the advantages of both: The SGA global method is

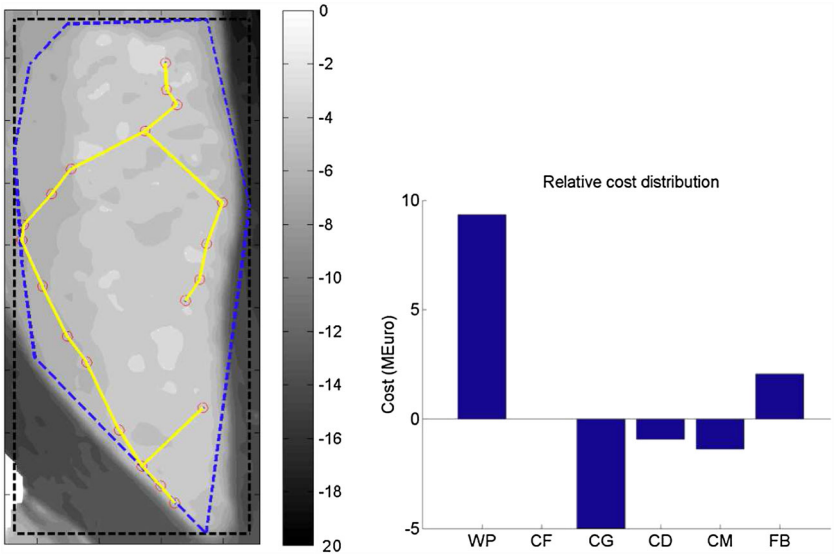

(a) Layout optimization result. The color scale indicates the water depth in meters.

(b) Relative cost compared with the baseline layout. WP: Electrical sales, CF: Foundations costs, CG: Electrical grid costs, CD: Degradation costs, CM: Maintenance costs, FB: Financial balance. Positive means that it increases the financial balance of the wind farm.

Figure 10. Middelgrunden simple genetic algorithm+sequential linear programming optimization result.

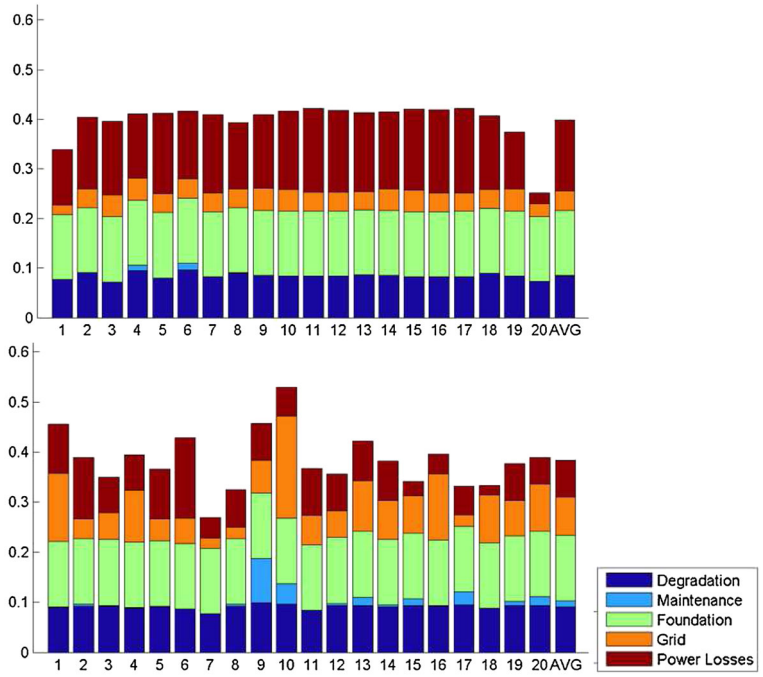

Figure 11. Financial balance elements for each turbine of Middelgrunden for the baseline layout (top) and the optimized layout (bottom).

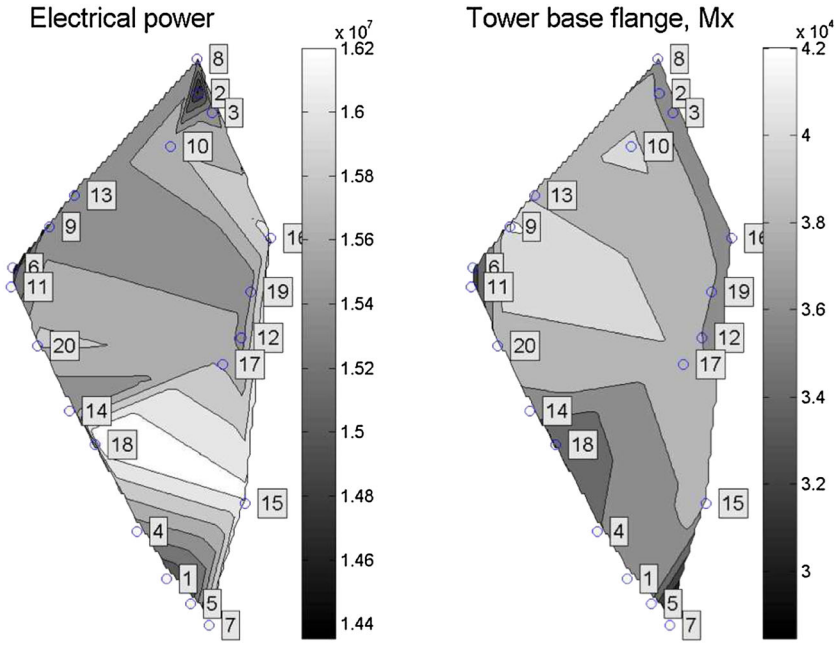

Figure 12. Simple genetic algorithm+sequential linear programming: Contour plots of electricity production [kWh] (left) and Tower base over turning bending moment (lifetime equivalent load [Nm]) (right).

not sensitive to local minima and can make use of a more clever and coarse design variable mapping; and the SLP method is efficient in refining the result and in handling of constraints.

The 2×3 fictitious test case also show how the different elements of the financial balance interact. It is clear that the foundation costs play a major role as the individual turbines are located in areas of shallow water. The somewhat arbitrary location of the baseline layout with some turbines located at large water depths makes it possible for the optimizer to

improve the financial balance significantly. The outcome of this specific optimization will therefore be strongly influenced by the foundation costs relatively to the other financial balance elements. For both 2×3 fictitious test case approaches, the optimizer exploit the potential for reducing the electrical grid costs without a significant change in the energy production. It is clear, that there is a trade off between electrical grid costs and energy production, as shorter cables imply that turbines are located closer to each other, which results in wake losses as well as increased loads from wake operation. Both the degradation costs and the O&M costs will increase when the distance between turbines reduces and therefore contribute to the trade off counteracting shorter electrical cables.

The result of the Stags Holt/Coldham test case were obtained after 1000 iterations by using the SGA algorithm and 30 iterations of the SLP algorithm. On this onshore test case, the foundation cost are assumed not variable and are therefore not considered to have an influence on the optimization. The two main drivers of the optimization are therefore the wake interaction of the turbine and the cabling price. This test case resulted in an improvement of the financial balance of 3.1 M€ (1.55 WTC). The improvement resulted from an increase in the energy efficiency together with cost reductions for electrical grid, turbine degradation, and O&M. This test case showed that the micro tailoring of the individual turbine locations leads to a significant improvement of the financial balance, and that the detailed wind climate information available is turned into an optimum position for each of the turbines. However, the wind resource spacial variation is an aspect neglected in this study. This aspect is usually much more pronounced onshore than offshore because of the frequent change in upstream local orography. Ideally, onshore wind farm optimization should be combined with a wind resource assessment tool such as WAsP,[32] to take this aspect into account.

The result of the Middelgrunden test case required 1000 iterations by using the SGA algorithm (level 1) followed by 20 SLP iterations (level 2) refining the optimized layout. The global SGA converges in steps due to the nature and principle of this algorithm. Convergence is very stable but slow, and after approximately 500 iterations, there appears to be only insignificant improvement of the objective function. The SLP algorithm runs subsequently for 20 iterations after which no further improvement of the solution seems possible with this algorithm. The 20 turbines result in 40 design variables and with constraints on turbine spacing and domain boundaries; the optimization problem is very complex.

The large difference for Middelgrunden between the financial balance after the SGA algorithm (level 1) and the financial balance after the SLP refinement (level 2) can be explained by the penalty function applied on the minimum distance between turbines in the SGA algorithm, which reduces the power production of the wind farm. Because of the local nature of the SLP algorithm, it is able to comply more efficiently with the constraint on the minimum distance by simply displacing the turbines too close to each others.

When looking at the solution of the Middelgrunden test case in Figure 10(a), it is fundamentally different from the baseline layout, in that the turbines are no longer arranged on line with a limited spacing between turbines. The resulting layout makes use of the entire feasible domain, and the turbines are not placed in a regular pattern. A closer look on the financial balance subelement changes in Figure 10(b) shows, that the foundation costs have not been increased because the turbines have been placed at shallow water in both configurations. The major changes involve energy production and electrical grid costs. Figure 11 shows the details of the financial balance elements for each of the turbines. A few turbines, for example, 9 and 10, have high O&M costs in contrast to the initial baseline layout, whereas most turbines have high annual energy efficiency. Turbine 10 has a relatively high energy production and a relatively high tower based flange moment, probably due to the wake meandering emitted from turbine 13 and 9. This illustrates that the fatigue loads can have an important influence on the financial balance, which would not be captured by an optimization purely on the basis of the power production.

Figure 12 shows how energy production (left) and lifetime equivalent tower base over-turning moment (right) change between the turbines in the wind farm. The dark areas in the left part of Figure 12 show turbines having comparatively lower energy production efficiency, and the light areas to the right show turbines with comparatively higher tower base loads. The fact that some of the turbines have comparatively high degradation and O&M costs is supported by the contour plot showing a few problem areas in the wind farm. Also a few problem areas appear for the energy production. The optimization result therefore leaves an open a question mark, on whether the global optimum was found. It is likely that adjustments in some of the areas in the wind farm can lead to further improvements of the financial balance, but it is not likely that a significant change in the value of the improvement is obtainable. Looking at the results, it cannot be excluded that the results can be improved with further iterations. When deciding on the final wind farm layout, it is therefore important to consider the local financial balance for each turbine and other factors that may influence decision making but are not present in the cost function. This could, for example, be power quality for the wind farm as a whole, where it might be desired to have a minimum variation of power with wind direction. The Middelgrunden test case emphasizes, that the trade off between electrical grid costs and energy production, degradation and O&M costs is decisive for the optimization result. The resulting improvement of the financial balance of 2.1 M€ (1.05 WTC) originates from a very large increase in the energy production value of 9.3 M€ (4.65 WTC) counterbalanced by mainly electrical grid costs. The optimization result is therefore sensitive to the cost modeling, and this stresses the importance for an accurate modelling of the electrical grid costs. It is therefore a weak point in the current work, that only little sophistication has gone into the modeling of electrical costs, where it is not considered that cables between clusters of turbines may be more expensive, and that costs for laying

down cables should depend on the local water depth conditions. A more sophisticated model, such as the one advocated by Elkinton,[5] could be considered in a future work.

A potentially important factor, which is not considered in the present analysis, is the variation of wind speed over the domain considered. Middelgrunden is located near the coast of Copenhagen, in a region where westerly wind undergo a rather dramatic roughness change. The consequence is that the wind speed would increase with the distance from the coast as it starts to recover from the effect of roughness change. In order to take this effect into account, it could be considered in further future work to couple the wind farm optimization platform with a wind speed estimation program such as WAsP.[32]

The meta-model used to describe the equivalent fatigue loads is based on a linear interpolation of a database of different wind turbine interaction cases. It is important to note that linear interpolation can introduce some discontinuity at the position of the data points, which can have a serious effect on gradient-based optimization such as SLP. This shortcoming could be addressed by using more advanced meta-model methods such as using a Kriging interpolation instead. Similarly, the norm used to constraint the SLP optimization (distance from the boundaries and minimum distance between the turbines) are not differentiable everywhere, which can potentially yield suboptimal performance of the SLP algorithm and even accelerate its convergence to a local minima. This should be the topic for a future work.

The multi-fidelity method investigated in this work is relatively simple, in the sense that the higher order models are used to refine the layout found by the lower order model. The errors made by the lower order model can therefore potentially lead the optimization to be captured in a local optimum. A better approach could be to use a more advanced multi-fidelity method, which are proven to converge towards an optimum of the higher order of fidelity models such as the one described in Robinson *et al*.[8]

Another important issue is the optimization approach. Clearly the use of a global method and a gradient-based method in combination has proved itself capable of finding an optimum solution. However, the slow convergence of the global method is an issue when going to larger wind farms, where calculation costs can become excessive. Tuning of the software implementation and switching to a faster platform than MATLAB can increase efficiency, and the use of parallel computing is likely to bring down the total simulation time significantly. Another issue is the use of the entire wind farm financial balance as optimization objective, because this allows a few turbines in the selected layout to have a comparatively poor turbine financial balance compared with the average of the wind farm. This can cause a need for manual tuning of the result and leaves open the question whether the solution is in fact global. Therefore, it should be looked into how the individual turbine financial balance can enter into the optimization objective function, possibly by optimizing on a subset of the wind farm or by composing the objective function differently and maybe making the number of wind turbine a design variable.

5. CONCLUSION AND FUTURE WORK

A wind farm optimization framework has been presented in details and demonstrated on three test cases. The results are over all satisfying and give some interesting insights on the pros and cons of the design choices. They show in particular that the inclusion of the fatigue load driven costs introduces some additional aspects in comparison with pure power based optimization. Further, refinement of the sensitive costs functions, especially the electrical grid costs, could result more realistic optimization results.

The multi-fidelity approach is found necessary and attractive to limit the computational costs of the optimization. Further improvement of the code, such as porting the MATLAB code to Fortran and parallelizing the optimization process should reduce dramatically the computational expense. This is needed in order to implement the last level of the multi-fidelity approach within the TOPFARM platform. Having an aero-elastic wind farm wake model in closed loop with a wind farm layout optimization would open the possibility to optimize the individual turbines components and control at the same time as the wind farm layout and the overall control.

ACKNOWLEDGEMENTS

This worked was financed by the EU-FP6 TOPFARM project contract no. TREN07/FP6EN/S07.73680/038641.

REFERENCES

1. Mosetti G, Poloni C, Diviacco B. Optimization of wind turbine positioning in large windfarms by means of a genetic algorithm. *Journal of Wind Engineering and Industrial Aerodynamics* 1994; **51**(1): 105–116. DOI: 10.1016/0167-6105(94)90080-9.
2. Beyer HG, Ruger T, Schafer G, Waldl HP. Optimization of Wind Farm Configurations with Variable Number of Turbines, *EUWEC, 20-24 May 1996*, Goteborg, Sweden, 1996.
3. Samorani M. The wind farm layout optimization problem. *Technical Report*, PowerLeeds School of Business, 2010.

4. Tesauro A, Réthoré PE, Larsen GC. State of the art of wind farm optimization, *EWEA*, Copenhagen, 2012.
5. Elkinton CN. *Offshore wind farm layout optimization*, PhD Thesis, University of Massachusetts Amherst, 2007.
6. Larsen GC, Madsen HA, Troldborg N, Larsen TJ, Réthoré PE, Fuglsang P, Ott S, Mann J, Buhl T, Nielsen M, *et al.* TOPFARM: next generation desigh tool for optimisation of wind farm topology and operation. *Technical Report, Risø-R-1805(EN)*, DTU Wind Energy, Ris, Roskilde, Denmark, 2011.
7. Larsen GC. A simple generic wind farm cost model tailored for wind farm optimization. *Technical Report, Risø-R-1710(EN)*, Risø DTU, Roskilde, Denmark, 2009.
8. Robinson TD, Eldred MS, Willcox KE, Haimes R. Surrogate-based optimization using multifidelity models with variable parameterization and corrected space mapping. *AIAA Journal* 2008; **46**(11).
9. Buhl T, Larsen GC. Wind farm topology optimization including costs associated with structural loading, *(TORQUE) The Science of Making Torque from the Wind, 3rd Conference*, Iraklion, Greece, 2010.
10. Réthoré PE, Fuglsang P, Larsen TJ, Buhl T, Larsen GC. Topfarm wind farm optimization tool, Risø DTU, Roskilde, Denmark, 2011.
11. Fuglsang P, Madsen HA. Optimization of stall regulated rotors. *ASME, SED* 1995; **16**: 151–158.
12. Fuglsang P, Madsen HA. Optimization method for wind turbine rotors. *Journal of Wind Engineering and Industrial Aerodynamics* 1999; **80**(1-2): 191–206. DOI: 10.1016/S0167-6105(98)00191-3.
13. Fuglsang P, Thomsen K. Site-specific design optimization of 1.52.0 MW wind turbines. *Journal of Solar Energy Engineering* 2001; **123**(4): 296. DOI: 10.1115/1.1404433.
14. Arora JS. *Introduction to Optimum Design*. Elsevier Academic Press: San Diego, CA, 2004.
15. Goldberg D. *Genetic Algorithms in Search, Optimization, and Machine Learning*, (1st edn). Addison-Wesley Professional: Reading, Massachusetts, 1989.
16. Goffe W, Ferrier G, Rogers J. Global optimization of statistical functions with simulated annealing. *Journal of Econometrics* 1994; **60**(1-2): 65–99. DOI: 10.1016/0304-4076(94)90038-8.
17. Veldkamp D. *Chances in wind energy, a probabilistic approach to wind turbine fatigue design*, PhD Thesis, Delft University, 2006.
18. Larsen GC, Madsen HA, Mann J, Bingöl F, Sørensen JN, Ott S, Okulov V, Troldborg N, Nielsen M, Thomsen K, *et al.* Dynamic wake meandering modeling. *Technical Report, Risø-R-1607(EN)*, Risø DTU, Roskilde, Denmark, 2007.
19. Larsen GC. A simple stationary semi-analytical wake model. *Technical Report, Risø-R-1713(EN) August*, Risø DTU, Roskilde, 2009.
20. Larsen GC, Madsen HA, Larsen TJ, Troldborg N. Wake modeling and simulation. *Technical Report, Risø-R-1653(EN)*, Risø DTU, Roskilde, Denmark, 2008.
21. Larsen GC, Madsen HA, Thomsen K, Larsen TJ. Wake meandering: a pragmatic approach. *Wind Energy* July 2008; **11**(4): 377–395. DOI: 10.1002/we.267.
22. Madsen HA, Larsen GC, Larsen TJ, Troldborg N, Mikkelsen R. Calibration and validation of the dynamic wake meandering model for implementation in an aeroelastic code. *Journal of Solar Energy Engineering* 2010; **132**(4): 041014. DOI: 10.1115/1.4002555.
23. Larsen GC. From solitary wakes to wind farm wind fields a simple engineering approach. *Technical Report, Risø-R-1727(EN)*, Risø DTU, Roskilde, Denmark, 2009.
24. Larsen TJ, Hansen AM. How 2 HAWC2, the user's manual. *Technical Report, Risø-R-1597*, DTU-Wind Energy, Risø, Denmark, 2007.
25. Bingöl F, Mann J, Larsen GC. Light detection and ranging measurements of wake dynamics part I: one dimensional scanning. *Wind Energy* 2010; **13**(1): 51–61. DOI: 10.1002/we.352.
26. Thomsen K, Madsen HA. A new simulation method for turbines in wake – applied to extreme response during operation. *Wind Energy* 2005; **8**: 35–47. DOI: 10.1002/we.130.
27. Larsen TJ, Hansen AM. Influence of blade pitch loads by large blade deflections and pitch actuator dynamics using the new aeroelastic code HAWC2, *EWEC Conference 2006*, Athens, 2006; 2–6.
28. Jonkman J, Butterfield S, Musial W, Scott G. Definition of a 5-MW reference wind turbine for offshore system development. *Technical Report February*, NREL, Golden, Colorado, USA, 2009.
29. Nieslony A. Rainflow Counting Algorithm – File Exchange – MATLAB Central.
30. Veldkamp D. Data for Stags Holt/Coldham wind farm. *Technical Report*, 2010.
31. Hansen KS. Definition of local wind climate for Middelgrunden, DK Deliverable D17: EU – TOPFARM. *Project Report, TopFarm, TREN07/FP6EN/S07.73680/038641*, DTU-MEK, Lyngby, Denmark, 2010.
32. DTU. Wasp - the wind atlas analysis and application program. [Online]. Available: www.wasp.dk [accessed on 2013].